Electronic Supplementary Material (ESI) for Journal of Materials Chemistry A.

Supporting information (SI)

Enhanced Activity, Durability and Anti-poisoning property of Pt/$W_{18}O_{49}$ for Methanol Oxidation with a Sub-stoichiometric Tungsten Oxide $W_{18}O_{49}$ Support

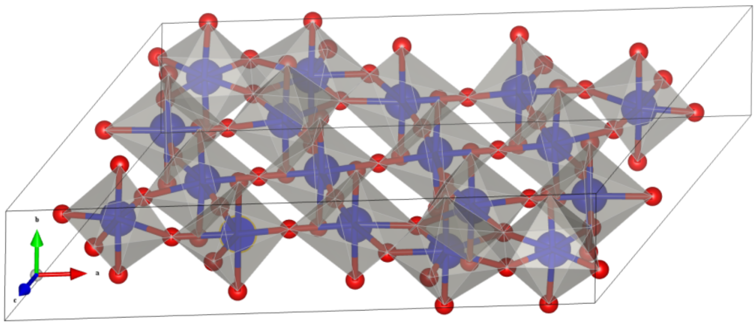

Fig. S1 Crystal structure of the monoclinic $W_{18}O_{49}$.

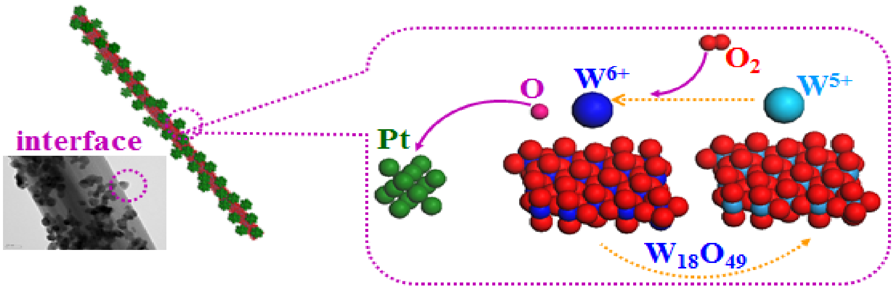

Fig. S2 Mechanism of the oxygen buffering effect in Pt/$W_{18}O_{49}$.

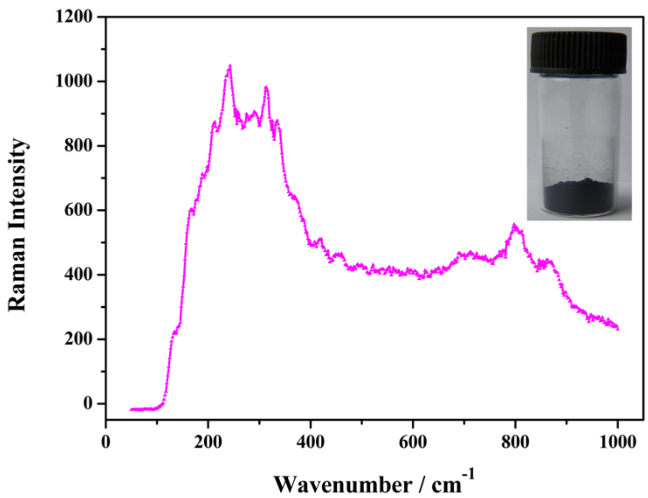

Fig. S3 Raman spectrum of the $W_{18}O_{49}$ nanowire arrays.

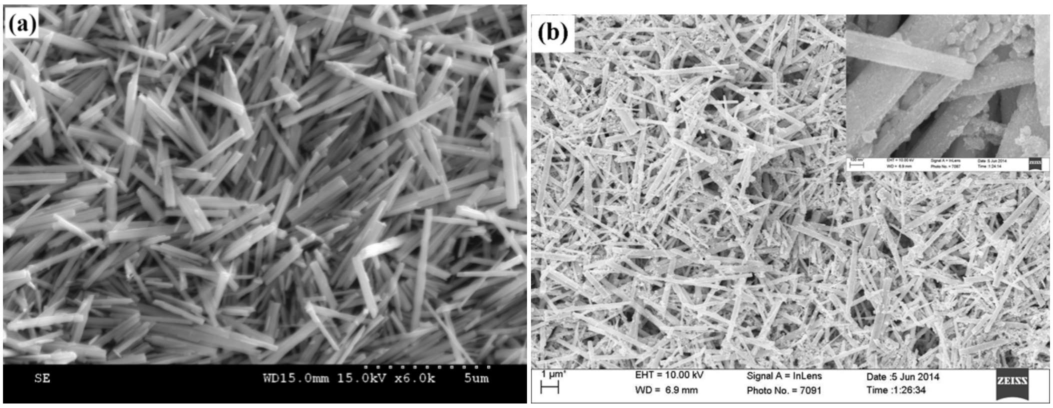

Fig. S4 SEM image of the (a) $W_{18}O_{49}$ NRs and (b) Pt/$W_{18}O_{49}$. High-magnification SEM image of Pt/$W_{18}O_{49}$ is shown in the inset of (b).

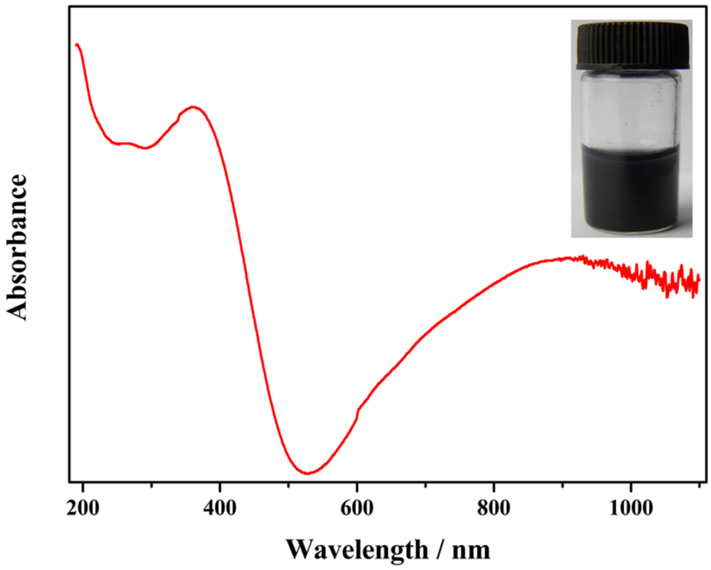

Fig. S5 Ultraviolet/visible (UV/Vis) absorption spectrum of the $W_{18}O_{49}$ NRs.

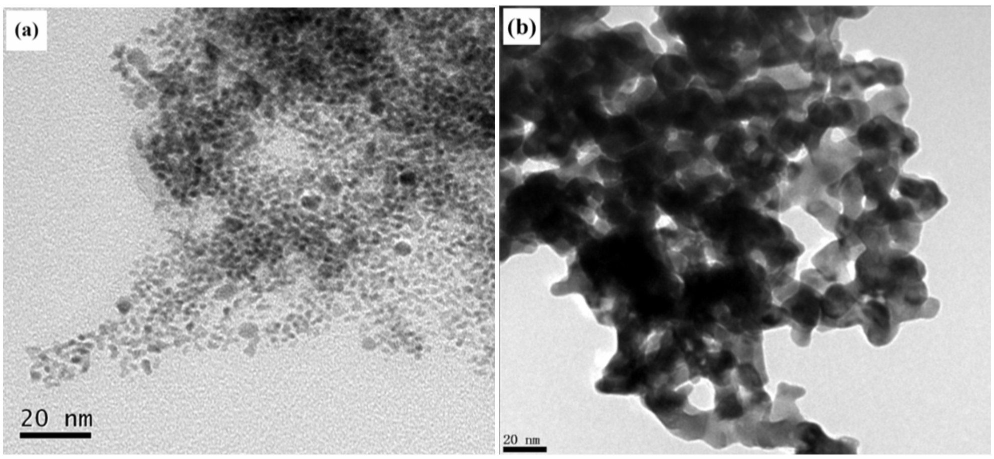

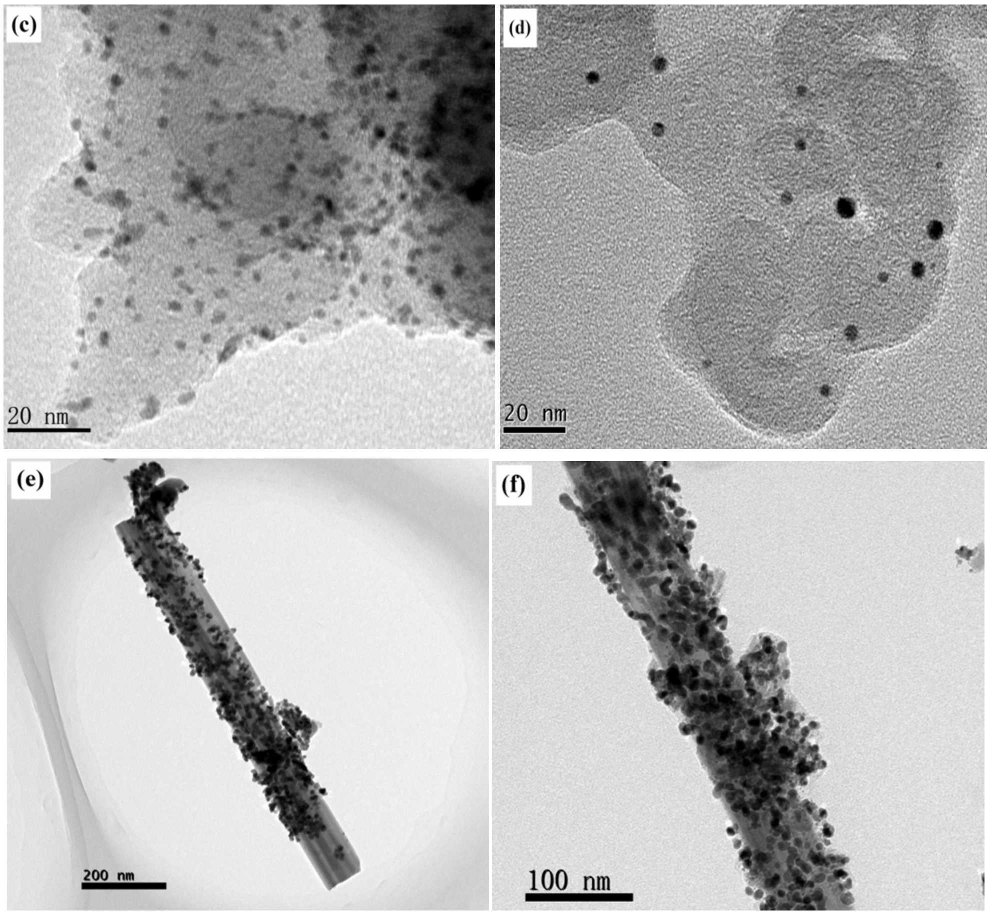

Fig. S6 TEM images of Pt-black: (a) dispersion before the durability test and (b) aggregation/Oswald ripening after a 5000-cycle durability test. Pt/C: (c) dispersion before the durability test and (d) dissolution/aggregation/Oswald ripening after a 5000-cycle durability test. Pt/$W_{18}O_{49}$: (e) dispersion before the durability test and (f) dispersion almost unchanged after a 5000-cycle durability test.

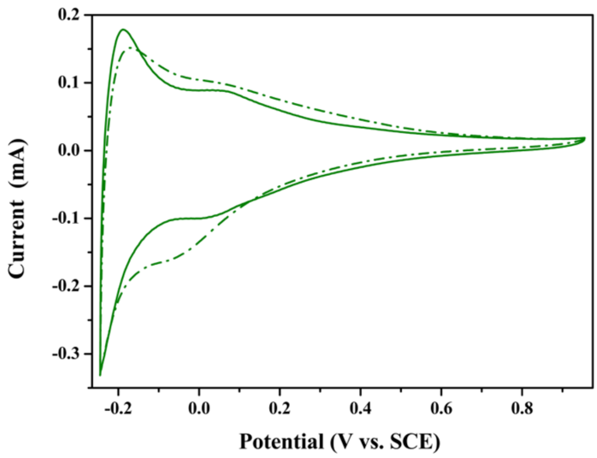

Fig. S7 ADT recorded in an Ar-purged 0.5 M H_2SO_4 with a sweep rate of 100 mV·s^{-1} of the $W_{18}O_{49}$ NRs support (solid for the1st cycle and dotted for the 5000th cycle).

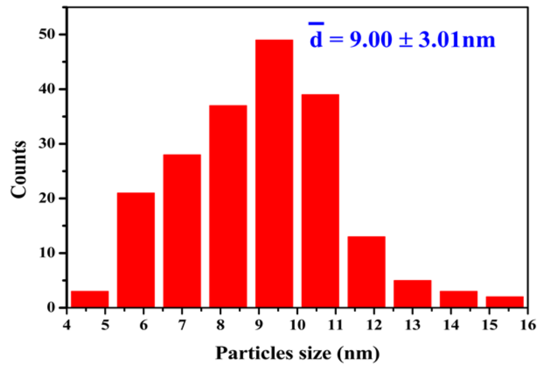

Fig. S8 The corresponding particle size distribution obtained by counting 200 Pt particles of Pt/$W_{18}O_{49}$ after a 5000-cycle ADT in Fig. S6f.

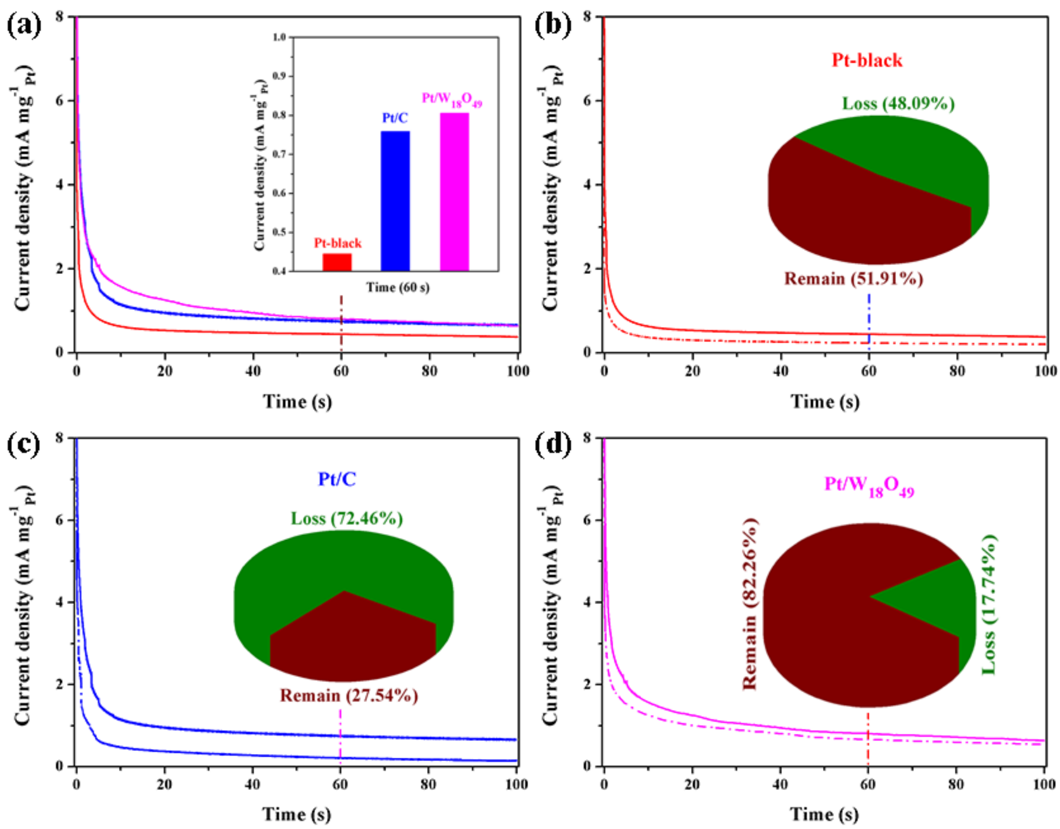

Fig.S9 Chronoamperometry measurements were performed in a 0.5 M $H_2SO_4$and 0.5 M CH_3OH solutionat 0.359 V (VS. SCE) after a 50-cycle CV activity in an Ar-purged 0.5 M H_2SO_4 solution with a sweep rate of 100 mV·s^{-1}. (a) Transient current density curves of methanol oxidation by chronoamperometry experiments for Pt/$W_{18}O_{49}$ (purple curve), Pt-black (red curve) and Pt/C (blue curve), the potential dependence of the steady-state current density recorded at 60 s is shown in inset. Chronoamperometry curves before and after a 5000-cycle ADT for Pt-black (red solid curve for the 1st cycle and dotted curve for the 5000th cycle in (b)) , Pt/C (blue solid curve for the 1st cycle and dotted curve for the 5000th cycle in (c)), Pt/$W_{18}O_{49}$ (purple solid curve for the 1st cycle and dotted curve for the 5000th cycle in (d)), inset is the loss of transient current density at 60 s after the ADT of the three catalysts, respectively.

Table S1 Binding energy and atomic content (%) of different W 4f valence states (W^{5+} and W^{6+}) obtained from the W 4f XPS spectra.

Sample		**W^{5+}**	**W^{6+}**
$W_{18}O_{49}$	Binding energy	33.90	35.64
	Content	26.22	73.78
Pt/$W_{18}O_{49}$	Binding energy	34.17	35.70
	Content	13.33	86.67
Pt/$W_{18}O_{49}$-CV	Binding energy	34.14	36.27
	Content	27.70	72.30

Table S2 Comparison of the electrochemical activities of the Pt/$W_{18}O_{49}$, Pt-black and Pt/C catalysts.

	onset potential (V)		**ECSA**		**Specific Activity (mA cm^{-2})**				
					CH_3OH			**HCOOH**	
	CH_3OH	**HCOOH**	**ECSA (m^2 g^{-1})**	**ECSA Loss (%)**	***I_f***	***E_f***	***I_f/I_b***	***I_f***	***E_f***
Pt-black	0.1	0.01	23.28	49.50	0.81	0.665	0.99	0.29	0.648
Pt/C	0.1	0.01	86.46	85.25	0.63	0.689	0.79	0.27	0.651
Pt-$W_{18}O_{49}$	0.1	0.01	37.05	27.12	1.14	0.654	1.12	0.44	0.656

Table S3 Comparison of the chronoamperometry activities of the Pt/$W_{18}O_{49}$, Pt-black and Pt/C catalysts at 0.359 V (Vs. SCE) before and after a 5000-cycle durability test at 60 s.

	Pt-black	**Pt/C**	**Pt-$W_{18}O_{49}$**
1th (mA mg^{-1}_{Pt})	0.445	0.759	0.806
5000th (mA mg^{-1}_{Pt})	0.231	0.209	0.663
Loss (%)	48.09	72.46	17.74